PHILOSOPHICAL TRANSACTIONS OF THE ROYAL SOCIETY A MATHEMATICAL, PHYSICAL & ENGINEERING SCIENCES

High Resolution Spectroscopy and Atmospheric and Stratospheric Detection of Minor Constituents with the Use of Tunable Spin Flip Raman Lasers

C. K. N. Patel

Phil. Trans. R. Soc. Lond. A 1979 **293**, 257-275
doi: 10.1098/rsta.1979.0095

Phil. Trans. R. Soc. Lond. A **293**, 257–275 (1979)
Printed in Great Britain

High resolution spectroscopy and atmospheric and stratospheric detection of minor constituents with the use of tunable spin flip Raman lasers

By C. K. N. Patel
Bell Laboratories, Murray Hill, New Jersey 07974, *U.S.A.*

With the advent of a variety of tunable infrared lasers, high resolution spectroscopy in this region has received a great boost. In particular the high power spin flip Raman laser is an excellent tool for very high resolution spectroscopy of ground state as well as excited states of molecules, saturation spectroscopy of molecules and two-photon Doppler-free spectroscopy of molecules. In addition, the use of opto-acoustic techniques for absorption measurements in conjunction with the spin flip Raman laser is capable of measuring absorption coefficients as small as 10^{-10} cm^{-1}. This ability has been of importance in the detection of minor constituents in the atmosphere and the stratosphere. This paper reviews some of these interesting investigations.

1. Introduction

Tunable infrared lasers have brought about a revolution in the area of molecular spectroscopy. The primary ingredients in this major change have been the high power and high resolution available from the variety of tunable infrared lasers which includes the tunable diode lasers,[1] the spin flip Raman lasers,[2] parametric oscillators,[3] and the colour centre lasers.[4] In addition, difference frequency as well as sum frequency mixing in nonlinear optical materials, together with tunable lasers such as the dye lasers,[5] the parametric oscillators in the visible or the near infrared region[6] or the spin flip Raman lasers,[7] has provided yet greater flexibility in the use of the tunable sources in the infrared region, defined here as a region that covers a wavelength range longer than about 2 μm. A comparison of the brightness (defined as flux per unit bandwidth per unit solid angle) of the radiation obtained from any of the above sources and that obtained from an infrared spectrometer employing state of the art black-body source yields the same orders of magnitude estimates which we obtain from comparison between other fixed-frequency lasers and black-body sources. Of the sources listed above, all but the diode lasers are secondary sources in that they require another fixed-frequency or tunable laser as a source or a pump. Thus the diode lasers represent a more convenient route to tunable laser radiation in the infrared; however, in general they are very low power devices, when especially compared with the spin flip Raman lasers and the parametric oscillators. Table 1

Table 1. Tunable infrared lasers†

laser	tuning range/μm	maximum power output/W		narrowest linewidth
		c.w.	pulsed	
parametric oscillator	up to 17	10^{-3}	10^{5} (100 mJ)	0.3 cm^{-1}
diode laser	up to 25	10^{-2}	100 (1 mJ)	100 kHz
colour centre laser	1.5–3.5	10^{-2}		
s.f.R. laser	3–17	2	10^{5} (10 mJ)	<1 kHz

† Infrared defined as $\lambda \geqslant 2.0$ μm

summarizes the general properties of these tunable sources in terms of the tuning range, power output and the measured smallest linewidth for each of them. Although the spin flip Raman laser represents perhaps the most recent entry into this field, it is characterized by very high continuous wave (c.w.) as well as pulsed tunable output powers. In the present paper, I will concentrate only on the spin flip Raman lasers and their applications to spectroscopy and other areas.

2. Description of spin flip Raman lasers

The advent of spin flip Raman lasers goes back to the discovery of high-power carbon dioxide[8] and other molecular lasers[9] providing intense radiation in the infrared. The discovery of the CO_2 laser and its subsequent development[10] resulted in extremely vigorous investigations of nonlinear optical effects in the 5–10 μm region.[11,12] Wolff[13] pioneered the idea of inelastic light scattering (Raman scattering) from the quantized cyclotron excitations of mobile carriers in semiconductors subjected to high magnetic fields. He showed that for electrons in InSb a Raman scattering process involving a change of Landau level quantum number of 2, given by

$$\omega_s = \omega_0 - 2\omega_c, \tag{1}$$

where ω_0 = frequency of the input radiation, ω_s is the frequency of the scattered radiation and $\omega_c = eB/m^*c$ is the cyclotron frequency of electrons in InSb, has a Raman scattering cross section of *ca.* 10^{-23} cm^2 sr^{-1} at $B \approx 5$ T. This led to a suggestion that with intense enough pump radiation at 10.6 μm a tunable magneto-Raman laser[14] could be obtained. Yafet[15] subsequently proposed another Raman scattering process with even larger cross section. This is the spin flip Raman (s.f.R.) scattering by mobile carriers in semiconductors in a magnetic field. This process is described by the equation

$$\omega_s = \omega_0 - g\mu B/\hbar, \tag{2}$$

where g is the g value of the electrons, μ_B is the Bohr magneton and B is the magnetic field. The s.f.R. cross section is approximately given by

$$\sigma_{\text{s.f.R.}} \approx \left(\frac{e^2}{m_s^* c^2}\right)^2 \left(\frac{\hbar\omega_0}{E_g}\right)^2 \left(\frac{E_g^2}{E_g^2 - (\hbar\omega_0)^2}\right)^2, \tag{3}$$

where m_s^* is the effective spin-mass of the electrons and E_g is the semiconductor bandgap. The last term in equation (3) represents the enhancement of cross section which occurs when the incident frequency approaches the bandgap. This term has turned out to be singularly important in obtaining c.w. stimulated spin flip Raman scattering. Non-enhanced s.f.R. cross sections were expected to be about 10^{-22} cm^{-2} sr^{-1} for InSb with a pump frequency at 10.6 μm.

Slusher *et al.*,[16] in their studies of narrow-bandgap semiconductors, observed the above two tunable spontaneous Raman scattering processes, together with a third process given by

$$\omega_s = \omega_0 - \omega_c, \tag{4}$$

whose strength was comparable to the $2\omega_c$ scattering process predicted by Wolff.[13]

The measured s.f.R. cross section[16] in InSb agreed well with the predictions, and this immediately led to the observation[17] that because of the large Raman scattering cross section and the small spontaneous scattering linewidth of the s.f.R. process, it was a prime candidate for obtaining a tunable laser in the infrared. The early studies of tunable s.f.R. Raman scattering in InSb were quickly extended to InAs[18] and PbTe.[19]

PHILOSOPHICAL TRANSACTIONS OF THE ROYAL SOCIETY A MATHEMATICAL, PHYSICAL & ENGINEERING SCIENCES

In spite of the apparent anticipated low threshold for obtaining s.f.R. laser action in InSb, it was in 1969 that Patel & Shaw[2] succeeded in the first demonstration of a tunable s.f.R. laser. The subsequent development of the field of s.f.R. lasers was extremely rapid.[20] Mooradian *et al.*[21] demonstrated c.w. operation at low threshold pump power by taking advantage of the resonance enhancement predicted by Yafet.[15] The next major step came with the recognition that because of the very densely spaced molecular laser lines for CO_2 and CO lasers (*ca.* 2 cm^{-1} spacing in CO_2 and *ca.* 4 cm^{-1} spacing in CO), the InSb s.f.R. laser can be made to cover a broad spectral region with a magnetic field of only *ca.* 0.2 T (because the effective g-value of electrons in InSb is *ca.* -50, resulting in a tuning rate $\delta(\omega_s)/\delta B$ of equation (2) of *ca.* 23.3 cm^{-1}/T). Patel reported this major development in 1971[22, 23] by using a very low carrier concentration InSb sample where tunability was extended to magnetic fields as low as 2×10^{-2} T. Instead of the superconducting solenoids used in the earlier experiments, ultrastable electromagnets (or permanent magnets) were used. Because of decreased linewidth and larger possible resonance enhancements, pump power thresholds as low as 1 mW at 5.3 μm were shown to be possible. In terms of very high resolution spectroscopy the low field operation represents a significant major step because of the magnetic field stability of the electromagnets. This development naturally led to the direct measurement of the linewidth of the s.f.R. laser output which, in Patel's first report,[24] was < 1 kHz limited by instrumental resolution. Brueck & Mooradian[25] have subsequently carried out measurements on the frequency stability. This is the narrowest linewidth of any of the tunable lasers mentioned in the Introduction.

TABLE 2. S.F.R. LASERS

material	pump laser	tuning range/μm	maximum power output/W	
			c.w.	pulsed
InSb	CO_2	9.2–15		10^5
InSb	CO	5.2–6.5	2	
InSb	doubled CO_2	5.2–6.5		100–1000
InSb	NH_3	13.5–16.8		1000
InAs	HF	3.2–3.3		100
$Hg_xCd_{1-x}Te$	CO_2	9–10.5	10^{-3}	
CdS	Ar	5145Å (± 8 mm^{-1})	10^{-3}	

The extension of s.f.R. lasers to other materials was also swift. InAs and CdS, in which spontaneous s.f.R. scattering had been reported earlier,[18, 26] were shown to exhibit s.f.R. laser action at appropriate pump wavelengths.[27, 28] An exciting development has been the observation of c.w. s.f.R. laser action in $Hg_{1-x}Cd_xTe$ in the 10 μm region[29] that was predicted[23] earlier. Table 2 summarizes the existing s.f.R. lasers, their pump wavelengths, tuning ranges, modes of operation and power outputs. A recent notable development[30] is the ability to use a long wavelength NH_3 laser[31] at 12.81 μm to pump the InSb s.f.R. laser which has yielded tunability in the 14–17 μm region (important for uranium isotope-separation schemes). PbTe is notably absent from the materials in which s.f.R. laser action has been seen, even though the observed spontaneous s.f.R. cross section and spontaneous s.f.R. linewidths are comparable[9] to those obtained in InSb. The reason for this is the lack of pump lasers at *ca.* 6.5 μm where one can take advantage of resonance enhancement. Powerful CO_2 lasers at 10.6 μm have not been successful because of the problems associated with multiphoton electron–hole plasma production[32] and the attendant increased free-carrier absorption. I am convinced that, with

PHILOSOPHICAL TRANSACTIONS OF THE ROYAL SOCIETY A MATHEMATICAL, PHYSICAL & ENGINEERING SCIENCES

proper pump wavelengths of 12.81 μm now available at power levels of *ca.* 750 kW [33] or s.h.g. at 6.4 μm at power levels of *ca.* 14 kW [34], s.f.R. laser action will be demonstrated shortly in PbTe and will serve to fill the conspicuous tuning gap for the s.f.R. lasers.

Since s.f.R. lasers are tuned by changing an externally applied magnetic field, and since the s.f.R. laser cavities are generally formed by the 'uncoated' endfaces of the laser crystal (see figure 1), the output frequency of the s.f.R. laser, in general, shows various amounts of non-linearity in its tuning characteristics described in equation (2). This nonlinearity, which is quite severe in InSb when pump wavelengths of *ca.* 10.6 μm are used, and relatively absent when a low-field modification is studied with pump at *ca.* 5.3 μm, arises from the mode pulling effects due to the s.f.R. gain curve sweeping past the fixed cavity resonances. This 'mode pulling' effect manifests itself into a modified s.f.R. laser tuning rate, $\delta\nu_L/\delta B$, given by

$$\frac{\delta\nu_{\mathrm{L}}}{\delta B} = \left\{\Delta\nu_{\mathrm{c}}\frac{\delta\nu_{\mathrm{s}}}{\delta B} - \frac{\nu_{\mathrm{s}}\Delta\nu_{\mathrm{spont}}}{n}\frac{\delta n(\nu_{\mathrm{L}}, B)}{\delta B}\right\} \Big/ \left\{\Delta\nu_{\mathrm{c}} + \Delta\nu_{\mathrm{spont}}\left[1 + \frac{\nu_{\mathrm{L}}}{n}\frac{\delta n(\nu_{\mathrm{L}}, B)}{\delta\nu_{\mathrm{s}}}\right]\right\}, \tag{5}$$

where $\Delta\nu_{\mathrm{c}}$ is the s.f.R. laser cavity linewidth, ν_{L} is the s.f.R. laser frequency, n is the refractive index of the s.f.R. laser crystal, ν_{s} is the s.f.R. gain line-centre frequency given by equation (2) and $\Delta\nu_{\mathrm{spont}}$ is the spontaneous s.f.R. scattering linewidth. Brueck & Mooradian [35] and Scragg & Smith [36] have recently used external cavity geometry for the s.f.R. laser which has allowed Scragg *et al.* to 'tune' the length of the s.f.R. laser cavity [37] to obtain an s.f.R. laser whose frequency tracks the s.f.R. tuning given by equation (2). This linearized tuning is bound to have significant impact on the practical design of s.f.R. lasers that use long-wavelength pumps at 10.6 μm or 12.81 μm where equation (5) predicts severe nonlinearity in the tuning characteristics. For the low field (and low concentration) InSb s.f.R. lasers pumped at 5.3 μm, the s.f.R. gain bandwidth $\Delta\nu_{\mathrm{spont}}$, first reported by DeSilets & Patel [38] and subsequently confirmed by Brueck & Mooradian [39] is very much smaller than $\Delta\nu_{\mathrm{c}}$, and equation (5) predicts a 99% or better tracking of s.f.R. laser frequency with that implied by equation (2).

In general, s.f.R. laser operation requires the s.f.R. crystal to be kept at low temperature for assuring that all the electrons occupy only the lowest spin substate and for obtaining the smallest possible spontaneous s.f.R. scattering linewidth. Typical crystal temperatures of 1–10 K are used and require liquid helium. DeSilets & Patel [38] have demonstrated that a closed-cycle refrigerator can equally well be used to keep the s.f.R. laser crystal at low temperatures. This development, together with the use of electromagnets for the magnetic field for tuning the s.f.R. laser frequency, has removed the need for any cryogenic fluids for the operation of the s.f.R. laser. Many dedicated or remotely located s.f.R. laser devices can now be used without close supervision.

It is not the theme of the present paper to describe in detail the operation of s.f.R. lasers; several reviews [20, 23] have been written on the subject. Operationally, the s.f.R. laser, as shown in figure 1, consists of a pump laser (see table 2), appropriate s.f.R. crystal in a cryogenic (or closed-cycle cooled) dewar and a source of magnetic field (a superconducting solenoid, electromagnet or a permanent magnet). The emerging radiation from the sample contains unconverted pump radiation as well as the s.f.R. laser radiation (Stokes, anti-Stokes in one or more orders). Restricting ourselves to the first Stokes s.f.R. laser, the s.f.R. laser radiation is easily separated from the unconverted pump radiation by using a polarizer since the polarization selection rules [15] are

$$(\epsilon_{0_x} + \mathrm{i}\epsilon_{0_y})\epsilon_{\mathrm{s}_z} + \epsilon_{0_x}(\epsilon_{\mathrm{s}_y} - \mathrm{i}\epsilon_{\mathrm{s}_z}), \tag{6}$$

PHILOSOPHICAL TRANSACTIONS OF THE ROYAL SOCIETY A MATHEMATICAL, PHYSICAL & ENGINEERING SCIENCES

where ϵ_0 and ϵ_s are the polarizations of the input and the s.f.R. scattered radiation, and the applied magnetic field B is parallel to z. Yafet[15] has shown that the second term of equation (6) i.e. $\epsilon_{0_z}(\epsilon_{s_x} - i\epsilon_{s_y})$ has a larger cross section than the first. Hence the geometry shown in figure 1 has k_0, k_s parallel to y where $k_{0,s}$ are the propagation vectors of the input and the s.f.R. scattered radiation respectively. With linearly polarized pump radiation along z, s.f.R. laser output will be polarized along x, i.e. normal to the pump radiation. Separation of the pump and s.f.R. laser is easily accomplished, with the use of an infrared polarizer.

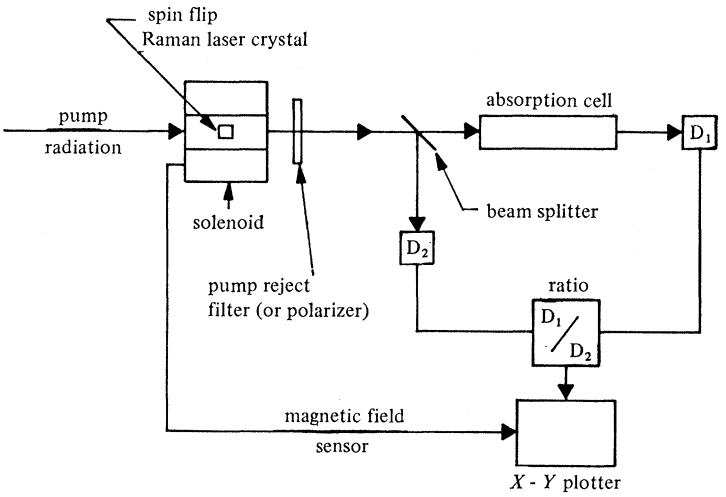

FIGURE 1. Schematic representation of a simple s.f.R. laser spectrometer.

3. SPECTROSCOPY AND OTHER APPLICATIONS OF S.F.R. LASERS

The advantages of using tunable laser radiation for high resolution spectroscopy are derived from the high power, monochromaticity and directionality which characterize the radiation. From the viewpoint of brightness all of the tunable lasers are far superior to a monochromator with a black-body source, and high power tunable laser sources possess special advantages of flexibility. This last point is especially appropriate in the infrared region where detectors, in general, have much poorer n.e.p. (noise equivalent power) compared to those in the visible spectral regions. Thus a quick look at table 1 convinces one that applications of s.f.R. lasers to spectroscopy hold much promise.

In the seven years since the first s.f.R. laser,[2] the spectroscopic capability of this new tunable source has been exploited by several groups in a variety of experiments. These have included straightforward spectroscopy of molecules, saturation spectroscopy, and two-photon Doppler-free spectroscopy as well as excited-state spectroscopy. In addition, the availability of the relatively high tunable powers has injected new life into an old spectroscopic tool, opto-acoustic spectroscopy.[40] This latter technique has now been developed to a point where it is capable of carrying out high resolution (Doppler limited) spectroscopy of gases at absorption levels as low as 10^{-10} cm^{-1}.

(a) *Molecular spectroscopy in the* 5 μm, 10 μm *and* 16 μm *regions*

Starting with initial results[41] on the use of the s.f.R. laser for spectroscopy of NH_3 at 10.6 μm, the s.f.R. laser has now been refined to carry out spectroscopy of NO in the 5 μm,[42,43,44] and

of UF_6 in the 16 μm region.[30] The arrangement shown in figure 1 is typical, but there have been several important technical developments which have to do with the specific nature of the source. For example, when using a pulsed s.f.R. laser, it is very important to ratio the transmitted signal and the reference signal on a pulse-to-pulse basis to account for pulse height fluctuations. Again for a pulsed s.f.R. laser source, it is important to make sure that the magnetic field tuning of the s.f.R. laser frequency is slow compared with the frequency scan between pulses and the structure that is to be resolved in the spectra of the molecules. For details of a well-designed s.f.R. laser spectrometer, the paper by Nowakowski[45] is recommended. Figures

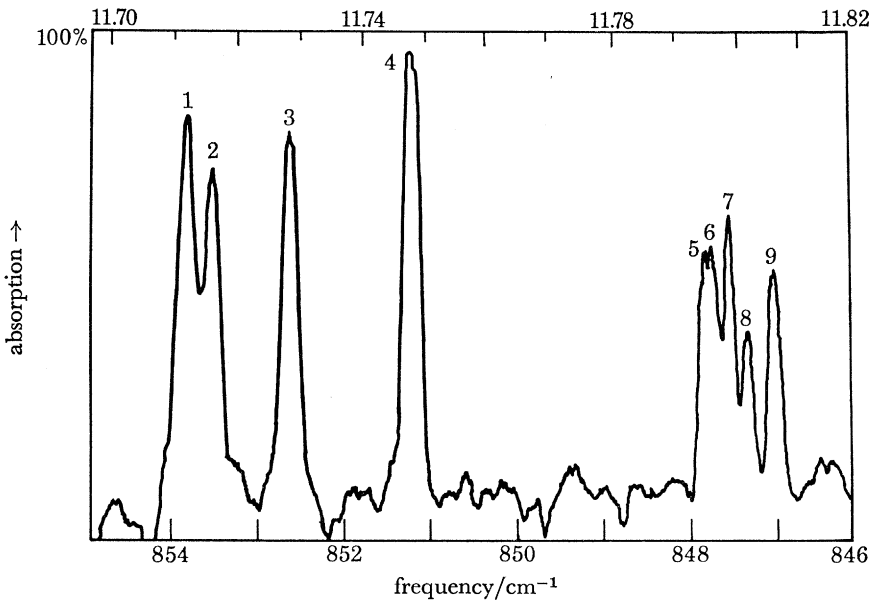

FIGURE 2. Absorption spectrum of NH_3 between 847 cm^{-1} and 854 cm^{-1} obtained with a pulsed CO_2 laser pumped InSb s.f.R. laser. P_{NH_3} = 10 Torr.

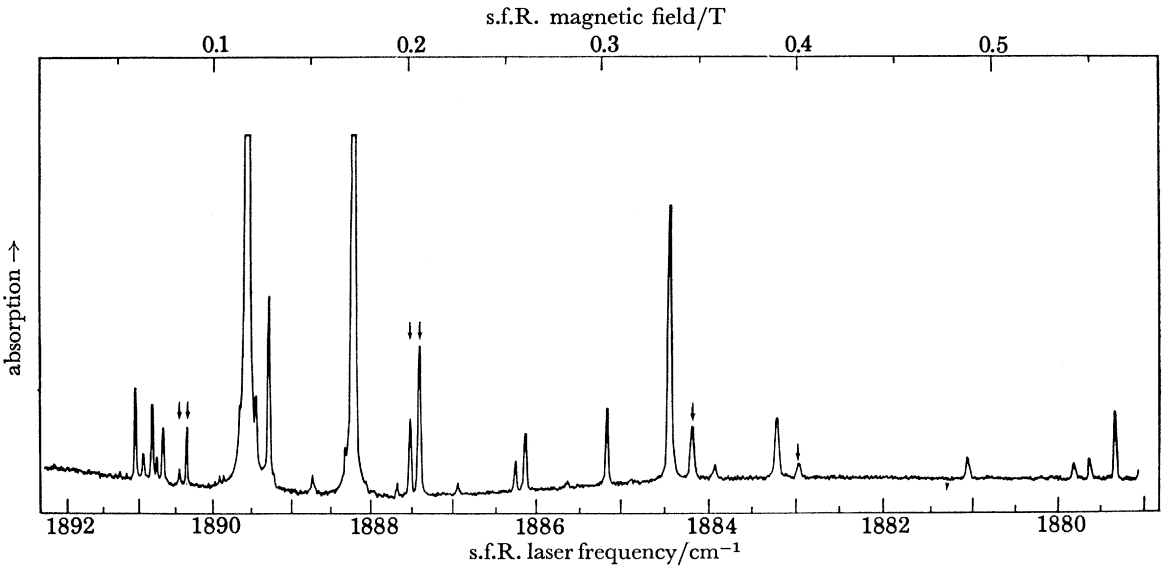

FIGURE 3. Absorption spectrum of 20/10^6 NO in N_2 between 1880 cm^{-1} and 1892 cm^{-1} obtained with a c.w. CO laser pumped low field s.f.R. laser. Pump laser at 1892.25 cm^{-1}, P = 76 Torr.

2, 3 and 4 show spectra of NH_3, 20 parts/10^6 NO in N_2, and UF_6 obtained in transmission spectroscopy in the 10.6 μm, 5.3 μm and 16 μm regions. In general, the resolution and quality of data available at 5.3 μm is better than that at either 10.6 μm or 16 μm because of the greater linearity of the s.f.R. laser frequency in the 5.3 μm operation of the low-field InSb s.f.R. laser. Straightforward transmission spectroscopy as well as modulation spectroscopy[46] of H_2O is shown in figure 5 where essentially Doppler-broadening-limited spectra are evident. Modulation spectroscopy with the s.f.R. laser is easily carried out by using modulation coils which provide a small time-varying magnetic field δB in addition to the magnetic field B needed for tuning the s.f.R. laser. Other s.f.R. laser spectroscopic studies include SbH_3, N_2O, OCS, HCOF, DBr and C_3H_6.[44,47]

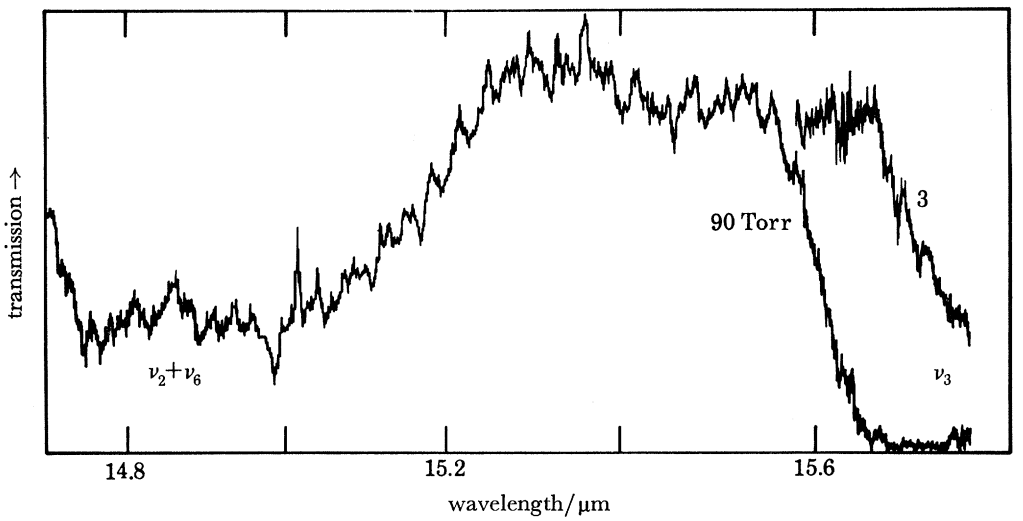

FIGURE 4. Absorption spectrum of UF_6 between 15.8 μm and 14.8 μm obtained with an NH_3 laser pumped pulsed s.f.R. laser.

(*b*) *Saturation spectroscopy with s.f.R. laser*

The limitation on the possible spectral resolution in the above experiments was set by the Doppler width at room temperature which for the H_2O spectrum shown in figure 5 is *ca.* 165 MHz. The s.f.R. laser has potentially a resolution of $\leqslant$ 1 kHz but may be limited in actual experiments by the frequency instability of the output. Some of this is easily avoided by using extensions of microwave techniques of frequency locking. To take advantage of the very narrow frequency width of the s.f.R. laser output, and to study spectral structure with widths narrower than Doppler width (e.g. natural width) use has been made of saturation spectroscopy (i.e. Lamb dip spectroscopy). Figure 6 shows an experimental Lamb dip arrangement using a low field s.f.R. laser.[48] In this experiment, the tuning magnetic field provided by the electromagnet was kept fixed and the fine tuning necessary to tune over a few hundred megahertz (*ca.* 5–10 × 10^{-4} T) is provided by a separate air-cored coil. It is here that the inherent advantages of the low-field development of InSb s.f.R. laser are obvious.

Figure 7 shows a saturation spectrum of the H_2O absorption line at 1889.54 cm^{-1} at a H_2O vapour pressure of 10 m Torr.† The observed Lamb dip has a width of *ca.* 200 kHz which includes contributions from the natural width, collisional width, the finite s.f.R. laser beam

† 1 Torr ≈ 133.322 Pa.

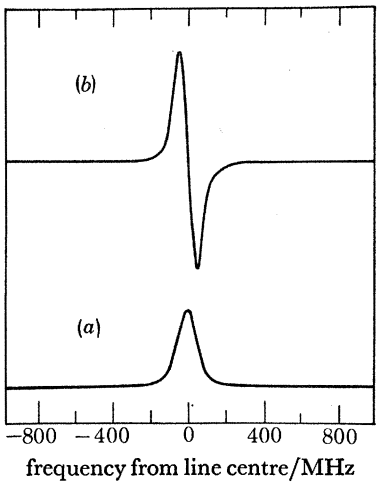

FIGURE 5. (*a*) Absorption and (*b*) derivative absorption spectrum of H_2O line at 1880.14 cm^{-1} obtained with a c.w. CO laser pumped low field s.f.R. laser.

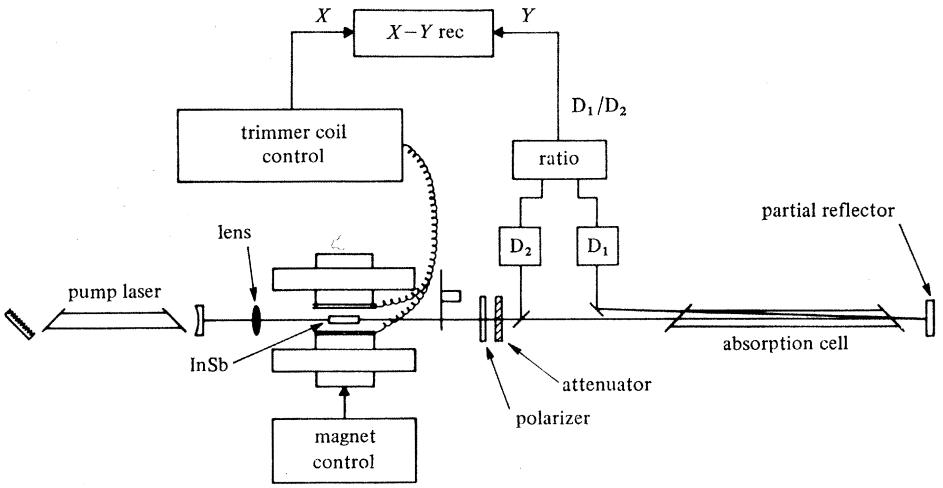

FIGURE 6. Experimental apparatus for saturation spectroscopy using an s.f.R. laser.

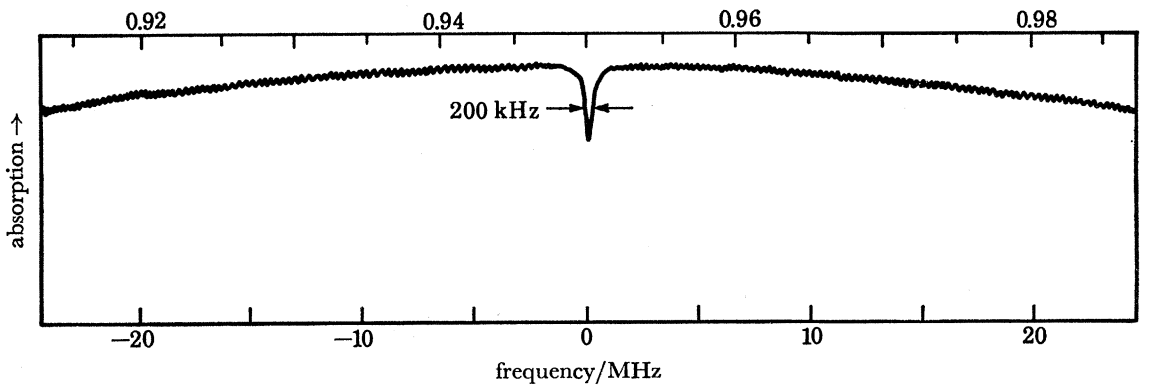

FIGURE 7. Lamb dip of H_2O. $P_{H_2O} \approx 10$ m Torr, $l \approx 40$ cm.

size of *ca.* 1 cm diameter, and lack of exact parallelism between the left and the right travelling waves. This homogeneous broadening amounts to about 100–150 kHz. The remaining broadening (*ca.* 100–150 kHz) comes from the frequency jitter of the s.f.R. laser output which had no locking provisions. The single mode s.f.R. laser output was approximately 100 mW and was attenuated before it entered the absorption cell, in order to keep the effects of power broadening to a minimum. However, it is seen that without the high c.w. s.f.R. laser power, saturation spectroscopy experiments would not be possible. For example, other c.w. tunable laser sources in the infrared do not provide enough power density in a large diameter beam.

While the saturation spectroscopy experiments to date have been carried out only on a simple molecular system, it is quite clear that extension to systems such as NO will allow a careful and detailed study of the nuclear hyperfine structure whose separation is much less than the Doppler width.[49]

(*c*) *Opto-acoustic spectroscopy*

In the above discussions of spectroscopic applications of the s.f.R. lasers, the absorption characteristics were determined by measuring the ratio of the input radiation intensity, I_{in}, and the transmitted radiation intensity, I_{out}. In this straightforward method of absorption measurements, the minimum measurable absorption in a sample is determined primarily by the fluctuations in the intensity of the input radiation, assuming that I_{in} as well as I_{out} is high enough not to be limited by the n.e.p. considerations of either of the detectors, D_1 or D_2 in figure 1. It is generally accepted that in this situation the smallest measurable absorption is *ca.* 10^{-4}, and that there is no dependence of the minimum absorption measurement on I_{in} (or I_{out}) as long as $I_{in}, I_{out} > 10^4$ (n.e.p.) of the detectors. In a modulated absorption measurement technique, instead of measuring the d.c. transmitted radiation intensity, we measure the time varying component. Again, as long as the n.e.p. of the detector is not a limiting factor, modulation spectroscopy yields a minimum detectable absorption of *ca.* 10^{-8} (i.e. for $I_{in} \geqslant 10^8$ (n.e.p.)). The dependence on the input intensity is *ca.* $(I_{in})^{-\frac{1}{2}}$; however, the limit of 10^{-8} is imposed by shot noise in the detector, beyond which no improvement is expected. The opto-acoustic (o.a.) technique, which is a calorimetric technique, relies on the measurement of $\Delta I = I_{in} - I_{out}$. Consider the excitation–de-excitation of an absorbing species (or atom) subjected to resonant radiation:

$$M + h\nu \longrightarrow M^* \text{ (excitation)}, \tag{7}$$

$$M^* \xrightarrow{k_{em}} M + h\nu \text{ (re-emission)}, \tag{8}$$

$$M^* \xrightarrow{k_{v-t}} M + kE \text{ (non-radiative de-excitation)}. \tag{9}$$

The operating principles of o.a. spectroscopy are easily understood for the case where the decay of the excited state is primarily through non-radiative processes – a case generally applicable to molecular absorption transitions in the infrared region because of the ν^3 dependence of the Einstein A coefficient for the transition. In this case, the energy of the excited molecular states appears as the translational energy of the molecules on de-excitation. This increase in kinetic energy of the molecules and consequential increase in the gas temperature manifests itself as an increase in the gas pressure (assuming a closed gas cell). For input radiation chopped at an audio frequency, the gas pressure is modulated at the audio frequency, which is effectively monitored by an acoustical transducer (e.g. ear, in the case of the first description of an o.a.

technique),[40] a capacitance manometer[50] or a capacitance microphone.[51] The experiments of Kreutzer & Patel[52] with a tunable s.f.R. laser source represented a key demonstration of the power of the o.a. technique for measuring small absorptions. In general, the detection sensitivity of the microphone is a predetermined quantity and thus the relation given by

$$P_{\min}(\text{transducer}) < I_{\text{in}}(1-\mathrm{e}^{-\alpha l}) \tag{10}$$

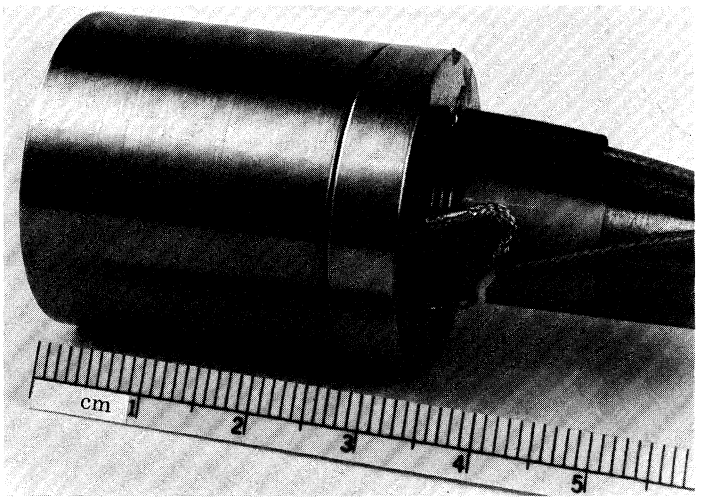

FIGURE 8. Miniature o.a. absorption cell.

governs the minimum detectability of the o.a. technique where $P_{\min}$ (transducer) is the equivalent n.e.p. (converted from the minimum detectable pressure change to absorbed optical power, taking into account among other factors the geometry of the apparatus), α is the absorption coefficient of the gas in cm^{-1}, and l is the path length. There are no obvious limitations on how small an α one can measure; however, the ultimate limitation is placed by spontaneous Raman scattering and Brillouin scattering which can convert the incident radiation frequency to a lower frequency. Details of this limitation will be published elsewhere.[53] The present results[54] show that with careful design and optimization, absorption coefficients as small as 10^{-10} cm^{-1} can be measured with tunable infrared power of *ca.* 100 mW available near 5 μm. It is at once clear that o.a. spectroscopy, in conjunction with a high-power tunable infrared laser such as an s.f.R. laser, constitutes a powerful tool for exploring very small absorption coefficients arising from (*a*) trace constituent gases in the atmosphere, (*b*) trace constituent gases in the stratosphere, (*c*) trace constituent gases in chemical reactions, (*d*) 'forbidden' absorption lines, (*e*) electric-field-induced, magnetic-field-induced, and pressure-induced absorption, (*f*) dimers, (*g*) excited state absorption, (*h*) Doppler-free multiphoton absorption, and (*i*) small quantities of isotopically substituted gases. The remainder of the paper describes some of the above studies.

(i) *High-resolution spectroscopy with opto-acoustic detection*

The ability to measure small absorption coefficients has led to construction of miniature opto-acoustic cells[54] (see figure 8) for spectroscopy of isotopically substituted gases. The total volume of the cell is approximately 2 cm^3. Using a low field c.w. s.f.R. laser pumped with a grating tunable CO laser we can scan frequencies from *ca.* 1850 cm^{-1} to 1895 cm^{-1} over which

the s.f.R. laser output is $\geqslant$ 100 mW. Figure 9 shows an opto-acoustic spectrum of ^{15}NO at a pressure of 200 m Torr obtained with a CO pump laser at 1897.6545 cm^{-1} $^{2\frac{1}{2}}(P_{8-7}(16)$ transition of CO). Λ-doubling of $R_{0-1}(\frac{2}{2}^{5})\Pi_{\frac{1}{2}}$ and $R_{0-1}(\frac{2}{2}^{1})\Pi_{\frac{1}{2}}$ is clearly seen. Table 3 lists the measured frequencies of $0 \rightarrow 1$ vibrational–rotational transitions of ^{15}NO in the $\Pi_{\frac{1}{2}}$ and $\Pi_{\frac{3}{2}}$ bands along with the first determinations of the Λ-doubling of ^{15}NO. These Λ-doubling data from $J = \frac{5}{2}$ to

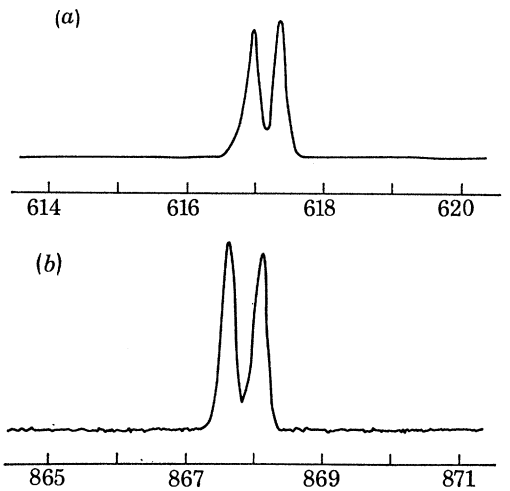

FIGURE 9. Opto-acoustic absorption spectra of ^{15}NO at 0.2 Torr showing Λ-doubling of the 0–1 $\Pi_{\frac{1}{2}}$ transitions; (*a*) $R_{0-1}(\frac{2}{2}^{5})\Pi_{\frac{1}{2}}$, (*b*) $R_{0-1}(\frac{2}{2}^{1})\Pi_{\frac{1}{2}}$.

$J = \frac{3}{2}^{3}$ allow a determination of the Λ-doubling parameters[55] p_Λ and q_Λ for the $v = 0$ and $v = 1$ state of ^{15}NO. Without going through the details of the analysis, preliminary studies yield

$$p_{\Lambda_0} = 170.16 \pm 1.74 \text{ MHz}, \tag{11a}$$

$$q_{\Lambda_0} = 1.17 \pm 0.33 \text{ MHz}, \tag{11b}$$

and

$$p_{\Lambda_1} = 168 \pm 2 \text{ MHz}, \tag{12a}$$

$$q_{\Lambda_1} = 1.00 \pm 0.4 \text{ MHz}. \tag{12b}$$

For details of these studies the reader is directed to Patel & Kerl.[56]

Other molecules studied by high resolution opto-acoustic spectroscopy include ^{14}NO,[57] OCS[47,58] N_2O,[47] and C_3H_6.[47] It is clear that with the advances in o.a. cells[54] where gas pressures as low as 20 mTorr can be used, o.a. spectroscopy with a high power tunable s.f.R. laser will continue to yield significant new results.

(ii) *Magneto-opto-acoustic spectroscopy*

Miniaturization of o.a. cells so that the gaseous molecules being investigated can be subjected to a high uniform magnetic field ($B \geqslant 10$ T) has allowed us to carry out Zeeman spectroscopy of ^{14}NO and ^{15}NO at fields up to 10.5 T, maintaining gas pressures low enough to contribute negligible collisional broadening. Figure 10 shows typical spectra of ^{14}NO at magnetic fields up to 8.6 T. Earlier Zeeman studies up to a magnetic field of *ca.* 5 T used conventional transmission measurement together with a diode laser.[59] For details of the analysis as well as Zeeman studies of ^{15}NO see Patel.[53] (The magneto-opto-acoustic technique has been used recently to study ^{14}NO with a fixed-frequency CO laser.[60])

TABLE 3. SUMMARY OF OBSERVED ^{15}NO TRANSITIONS: $0 \rightarrow 1$ VIBRATIONAL–ROTATIONAL BAND

band	$\nu_{observed}$ cm^{-1}	$\nu_{calculated}$† cm^{-1}	identification	Λ-doubling MHz
$\Pi_{\frac{1}{2}}$	1854.073	1854.08	$R_{0-1}(\frac{5}{2})$	377 ± 30
	1857.165	1857.159	$R_{0-1}(\frac{7}{2})$	347 ± 25
	1860.238	1860.208	$R_{0-1}(\frac{9}{2})$	350 ± 35
	1863.225	1863.222	$R_{0-1}(\frac{11}{2})$	380 ± 10
	1866.219	1866.207	$R_{0-1}(\frac{13}{2})$	342 ± 30
	1869.206	1869.157	$R_{0-1}(\frac{15}{2})$	329
	1872.160	1872.074	$R_{0-1}(\frac{17}{2})$	
	1875.030	1874.958	$R_{0-1}(\frac{19}{2})$	315
	1877.768	1877.809	$R_{0-1}(\frac{21}{2})$	285 ± 8
	1880.643	1880.628	$R_{0-1}(\frac{23}{2})$	290 ± 28
	1883.472	1883.412	$R_{0-1}(\frac{25}{2})$	262 ± 14
	1886.215	1886.164	$R_{0-1}(\frac{27}{2})$	261 ± 10
	1888.865	1888.882	$R_{0-1}(\frac{29}{2})$	
	1891.562	1891.567	$R_{0-1}(\frac{31}{2})$	240 ± 10
	1894.201	1894.218	$R_{0-1}(\frac{33}{2})$	240 ± 50
$\Pi_{\frac{3}{2}}$	1854.166	1854.168	$R_{0-1}(\frac{5}{2})$	
	1875.338	1857.330	$R_{0-1}(\frac{7}{2})$	
	1860.440	1860.457	$R_{0-1}(\frac{9}{2})$	
	1863.554	1863.550	$R_{0-1}(\frac{11}{2})$	
	1866.628	1866.605	$R_{0-1}(\frac{13}{2})$	
	1869.689	1869.626	$R_{0-1}(\frac{15}{2})$	
	1872.604	1872.610	$R_{0-1}(\frac{17}{2})$	
	1875.611	1875.559	$R_{0-1}(\frac{19}{2})$	
	1878.443	1878.471	$R_{0-1}(\frac{21}{2})$	
	1881.371	1881.348	$R_{0-1}(\frac{23}{2})$	
	1884.240	1884.188	$R_{0-1}(\frac{25}{2})$	
	1889.733	1889.752	$R_{0-1}(\frac{29}{2})$	
	1892.474	1892.486	$R_{0-1}(\frac{31}{2})$	

† Calculated values obtained by using Keck's[55] data.

(iii) *Excited state opto-acoustic spectroscopy*

Generally, at room temperature only the low lying vibrational–rotational states of molecules are populated and the spectroscopic studies of absorption starting from excited states is difficult. For example, in ^{14}NO where the $v = 1$ level is 1970 cm^{-1} above the ground state, the fractional population in the $v = 1$ level is *ca.* 10^{-4}. With the high sensitivity available when using the o.a. technique for absorption measurements, we are able to measure the excited-state absorption easily.[53] A more elegant approach to excited state absorption spectroscopy (e.s.a.s.) is to provide a means of increasing the population of the $v = 1$ state of NO (say) by selective excitation of $v = 0$ molecules with a second laser source. This technique for e.s.a.s. was first used with conventional absorption measurement techniques.[61] When the o.a. technique is coupled with e.s.a.s. the experiment simplifies considerably[62] since very short path lengths can be used, and hence the exciting beam and the probing beam do not have to remain collinear and focused over long distances. This requirement imposed, in the conventional absorption technique, the use of a 60 cm long optical waveguide[61] whose walls clearly provide, significant de-excitation as well as collisional broadening. Such problems do not exist with the o.a. technique when applied to e.s.a.s. Figure 11 shows the experimental arrangement used for studying e.s.a.s. of ^{14}NO and ^{15}NO. The fixed-frequency CO laser at 1917.8611 cm^{-1} ($P_{8-7}(11)$

PHILOSOPHICAL TRANSACTIONS OF THE ROYAL SOCIETY A MATHEMATICAL, PHYSICAL & ENGINEERING SCIENCES

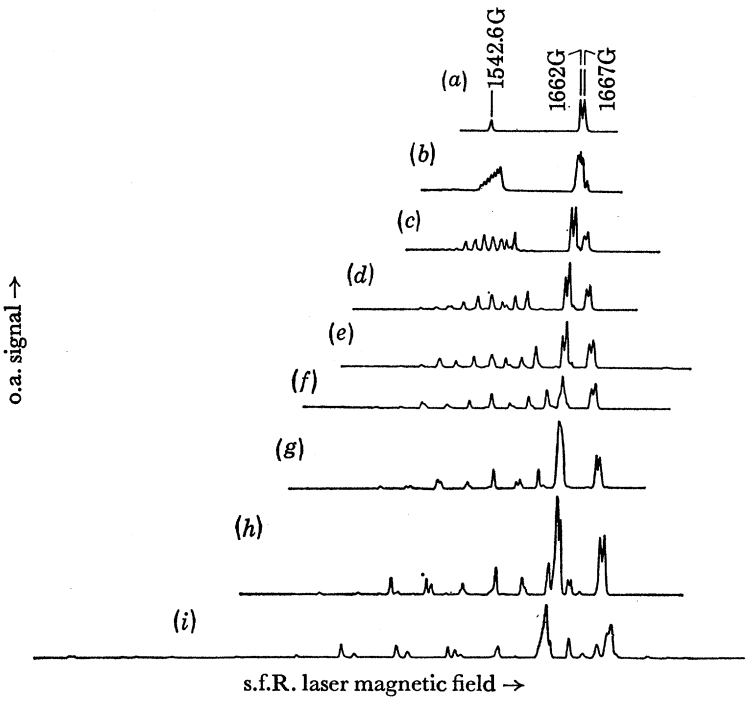

FIGURE 10. Opto-acoustic Zeeman spectra of ^{14}NO at 1 Torr, $R_{0-1}(\frac{13}{2})$ transition: (*a*) 0 T, (*b*) 0.662 T, (*c*) 1.888 T, (*d*) 2.982 T, (*e*) 3.675 T, (*f*) 4.507 T, (*g*) 5.438 T, (*h*) 6.268 T and (*i*) 8.585 T. $\nu_0 = 1896.17\ cm^{-1}$, $P_{9-8}(10); J = \frac{13}{2}$.

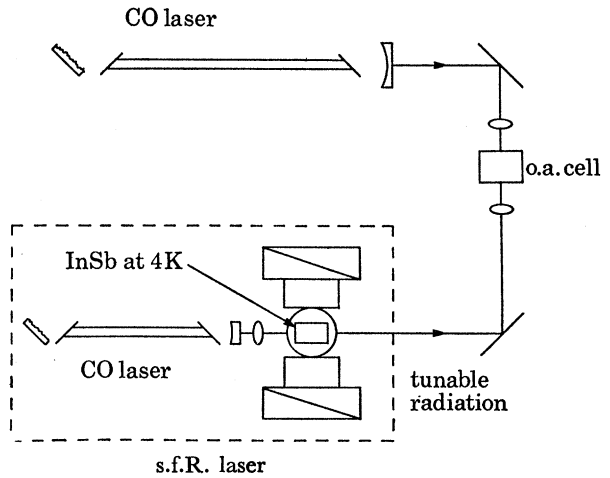

FIGURE 11. Experimental apparatus for excited state o.a. absorption spectroscopy.

transition) excites ^{14}NO to $v = 1$ levels through its accidental coincidence with the $R_{0-1}(\frac{27}{2})\Pi_{\frac{1}{2}}$ NO transition. The s.f.R. laser probes the $v = 1 \rightarrow 2$ o.a. absorption of ^{14}NO. Figure 12 shows a typical spectrum[62] in the region of 0.2–0.35 T. Table 4 summarizes data on the observed $\Pi_{\frac{1}{2}}$ and $\Pi_{\frac{3}{2}}$ $v = 1 \rightarrow 2$ transitions of ^{14}NO along with the first measurements of Λ-doubling of $v = 1 \rightarrow 2$ transitions. Excitation to the $v = 1$ state of $\Pi_{\frac{3}{2}}$ ^{14}NO arises through collisional vibrational energy transfer,

$$NO^*(v = 1, \Pi_{\frac{1}{2}}) + NO(v = 0, \Pi_{\frac{3}{2}}) \rightarrow NO(v = 0, \Pi_{\frac{1}{2}}) + NO^*(v = 1, \Pi_{\frac{3}{2}}), \qquad (13)$$

because the $v = 1$ levels of the $\Pi_{\frac{1}{2}}$ and $\Pi_{\frac{3}{2}}$ states are very close in energy. A point that is crucial here is that the excitation of ^{14}NO to $v = 1$ is very selective and no measurable increase in the molecular translational or rotational temperature is seen, ruling out any possibility of thermal heating of the gas being the primary cause of excitation of ^{14}NO molecules to $v = 1$.

Collisional energy transfer, which is selective in energy discrepancy between the initial and final configurations, has been further used[64] to study $v = 1 \rightarrow 2$ transitions of ^{15}NO. The o.a. cell now contains a mixture of ^{14}NO and ^{15}NO. The arrangement is unchanged from figure 11. Excitation occurs to the $v = 1$ level of ^{14}NO (because no obvious accidental match between the ^{15}NO $v = 0 \rightarrow 1$ transition and a CO laser transition exists). Molecular energy transfer,

$$^{14}NO^*(v = 1) + {}^{15}NO(v = 0) \rightarrow {}^{14}NO(v = 0) + {}^{15}NO^*(v = 1) \pm \Delta E, \qquad (14)$$

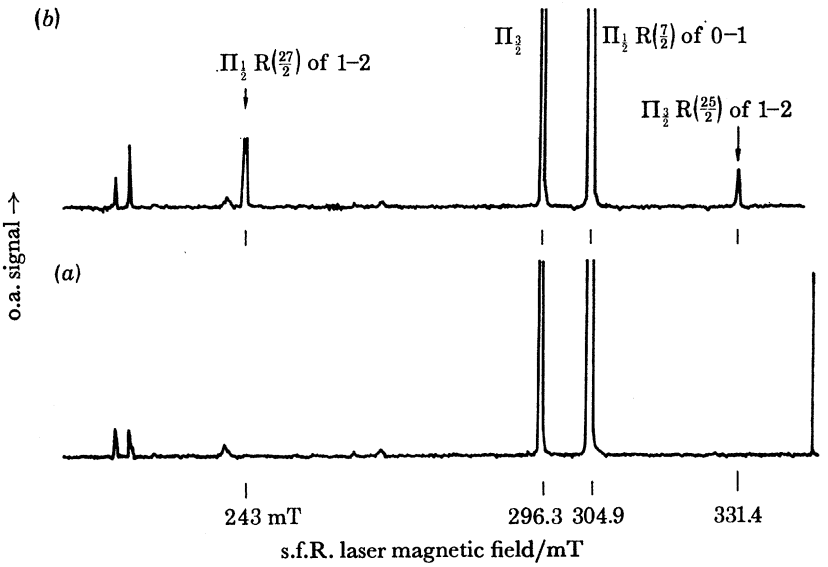

FIGURE 12. Excited state o.a. absorption spectra of ^{14}NO: (*a*) Without excitation from $v = 0$ to $v = 1$ level, and (*b*) with excitation from $v = 0$ to $v = 1$ level caused by the CO laser at 1917.88 cm^{-1}.

TABLE 4. $v = 1 \rightarrow 2$ TRANSITIONS OF ^{14}NO

	$\Pi_{\frac{1}{2}}$				$\Pi_{\frac{3}{2}}$		
J	observed	Amiot[63]	difference	Λ-doubling MHz	observed	Amiot[63]	difference
1.5	1856.088	1856.12	−0.032		1856.088	1856.138	−0.05
2.5	1859.324	1859.323	0.001	345 ± 15	1859.43	1859.414	0.016
3.5	1862.477	1862.478	−0.001	328 ± 17	1862.664	1862.598	−0.066
4.5	1865.613	1865.598	−0.015	340 ± 35	1865.877	1865.857	0.020
5.5	1868.733	1868.685	0.048	339 ± 35	1869.081	1869.022	0.059
6.5	1871.831	1871.736	−0.095	338 ± 15	1872.246	1872.15	0.099
7.5	1874.771	1874.753	0.018	312 ± 15	1875.203	1875.24	−0.037
8.5	1877.713	1877.736	−0.023	302 ± 18	1878.271	1878.292	−0.021
9.5	1880.681	1880.684	0.003	291 ± 40	1881.349	1881.305	0.044
10.5	1883.633	1883.596	0.037	300 ± 50	1884.299	1884.281	0.018
11.5	1886.462	1886.474	−0.012	275 ± 35	1887.200	1887.218	−0.018
12.5	1889.275	1889.316	−0.041	275 ± 35	1890.088	1890.116	−0.028
13.5	1892.115	1892.123	−0.008	236 ± 30	1892.960	1892.976	−0.016
14.5	1894.883	1894.895	−0.012	227 ± 35	1895.748	1895.796	−0.048
15.5	1897.611	1897.631	−0.02	240 ± 35			

PHILOSOPHICAL TRANSACTIONS OF THE ROYAL SOCIETY A MATHEMATICAL, PHYSICAL & ENGINEERING SCIENCES

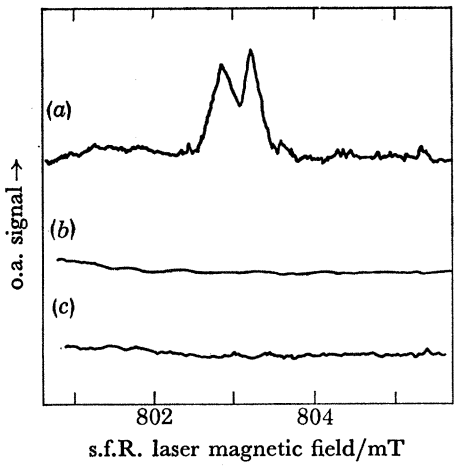

FIGURE 13. Excited state o.a. spectra of ^{14}NO: (*a*) With $^{14}NO + {}^{15}NO$ in the o.a. cell, and the CO laser at 1917.88 cm^{-1} present, (*b*) with $^{14}NO + {}^{15}NO$ in the o.a. cell, and the CO laser off, and (*c*) with ^{15}NO in the o.a. cell, and CO laser on.

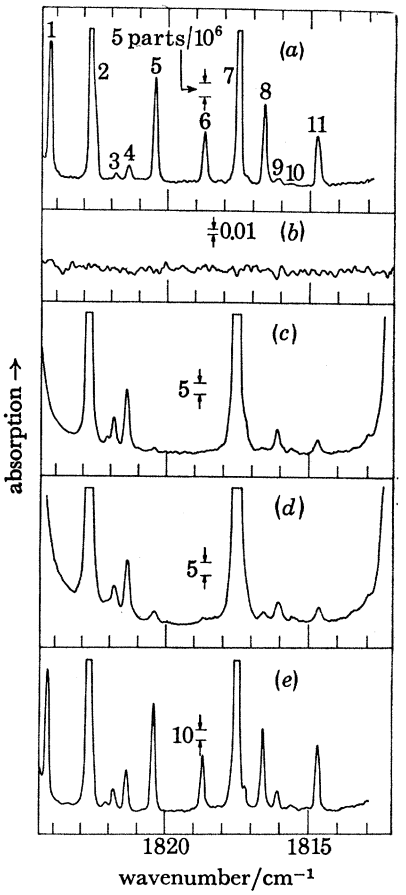

FIGURE 14. NO pollution detection with a s.f.R. laser–o.a. spectrometer: (*a*) 20 parts/10^6 NO calibration sample, (*b*) o.a. cell noise, (*c*) room air, (*d*) air sample from near a highway, and (*e*) effluent from a vehicle exhaust.

TABLE 5. SUMMARY OF OBSERVED ^{15}NO TRANSITIONS 1–2 VIBRATIONAL–ROTATIONAL BAND

band	$\nu_{observed}$ cm^{-1}	$\nu_{calculated}$† cm^{-1}	identification	Λ-doubling MHz
$^2\Pi_{\frac{1}{2}}$	1855.93	1896.02	$R_{1-2}(\frac{25}{2})$	350 ± 70
	1879.22	1879.19	$R_{1-2}(\frac{43}{2})$	280 ± 45
	1881.54	1881.58	$R_{1-2}(\frac{45}{2})$	
$^2\Pi_{\frac{3}{2}}$	1877.69	1877.71	$R_{1-2}(\frac{41}{2})$	
	1885.08	1885.07	$R_{1-2}(\frac{47}{2})$	

† Calculated values obtained by using (*a*) Keck's[55] rotational constants for $v = 1$, (*b*) Olman's[65] rotational constants for $v = 2$, and (*c*) vibrational band centre frequencies $\nu_{1-2}(^2\Pi_{\frac{1}{2}}) = 1815.98 \pm 0.7$ cm^{-1} and $\nu_{1-2}(^2\Pi_{\frac{3}{2}}) = 1815.71 \pm 0.07$ cm^{-1}.

provides a good selective excitation process for obtaining $^{15}NO^*$ ($v = 1$) because the energy discrepancy ΔE is small compared with kT at room temperature. The o.a. spectrum in figure 13 convinces one that the signal seen arises from e.s.a.s. of ^{14}NO. In spite of the need for collisions for obtaining $^{15}NO^*(v = 1)$ molecules, Λ-doubling is still evident. Table 5 summarizes the e.s.a.s. data for ^{15}NO. From the strength of the observed e.s.a.s. signals for ^{14}NO and ^{15}NO, specific collisional transfer rates have also been obtained.[64]

Since the o.a. cells in our present experiments are compatible with high field Zeeman studies (see above), we have carried out preliminary Zeeman spectroscopy of the $v = 1 \rightarrow 2$ transition of ^{14}NO and ^{15}NO.[62,66]

(iv) *Measurement of trace constituents in the atmosphere*

Kreuzer & Patel in their 1971 paper[52] introduced the use of the tunable s.f.R. laser o.a. absorption measurement technique for detection and quantitative determination of densities of trace constituents in the atmosphere (i.e. pollution detection). The high resolution afforded by the s.f.R. laser allows us to obtain a 'fingerprint' absorption of the desired trace gas without any interference from other gases. A typical example is NO, which is a common industrial as well as automotive effluent. Its infrared absorption (see §(i) above) in the 5.3 μm region is closely surrounded by strong H_2O absorption lines as seen in figure 3. Because of the resolution available, we are able to isolate and identify the NO absorption lines and hence measure the NO concentration. Figure 14 shows data on a 20 parts/10^6 NO calibration sample, ambient NO in a laboratory, ambient NO near a highway and vehicle exhaust NO emission. One is immediately struck by the wide dynamic range afforded by the s.f.R. laser–o.a. measurement technique. With the recent advances in microphone construction,[54] we are able to detect as few as 10^7 NO molecules cm^{-3} (a volumetric mixing ratio of better than $1 : 10^{12}$ at atmospheric pressures). With the same technique, NO concentrations as high as 10^{16} cm^{-3} can be measured (volumetric mixing ratio of *ca.* $1 : 10^3$ at atmospheric pressure). The o.a. technique yields signals which are linear in NO concentration over the 9 orders of magnitude variation. The nonlinearity at the high concentration end arises from absorption in the o.a. cell becoming large enough to give a significant variation of the probe radiation intensity as it traverses the o.a. cell. At the low end, we are limited by microphone noise, absorption in the optical windows and finite tunable s.f.R. laser power output.[53]

(v) *Measurements of trace gaseous constituents in the stratosphere*

The ability to measure NO concentrations as low as 10^7 molecules cm^{-3} has found an exciting application. Nitrogen oxides are known and expected to play an important role in the ozone chemistry in the stratosphere,[67,68] through their catalytic destruction of ozone. While the principal source of NO and NO_2 in the stratosphere so far has been the dissociation by ^1D oxygen atoms of the upwardly diffused N_2O, there is concern about the possibility of upsetting the natural balance through the direct injection of NO and NO_2 into the stratosphere by high-flying aircraft. Since the catalytic destruction of ozone (*ca.* 10^{12} cm^{-3} at 28 km) by NO and NO_2 (*ca.* 10^9 cm^{-3} at 28 km) is strongly governed by solar radiation, it is imperative that the validation of the catalytic destruction of ozone by NO and NO_2 involve a measurement not only of NO (or equivalently NO_2) concentration but also of its diurnal variation.[69] Starting with the first balloon-borne s.f.R. laser–o.a. measurements in 1973 we have obtained the

PHILOSOPHICAL TRANSACTIONS OF THE ROYAL SOCIETY A MATHEMATICAL, PHYSICAL & ENGINEERING SCIENCES

required information on NO kinetics (and hence on the ozone catalytic destruction cycle). This is summarized in figure 15. Recent measurements by Chaloner *et al.*[70] have provided confirmation of the 1973 and 1974 measurements.[(69)]

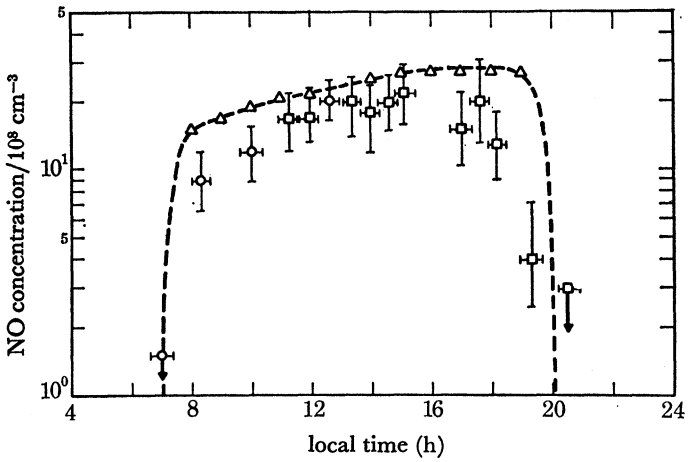

FIGURE 15. Time variation of NO concentration in the stratosphere obtained with a balloon-borne s.f.R. laser–o.a. spectroscopy system. ○, Autumn 1973 data; □, Spring 1974 data; —△—, Johnson calculations.

4. CONCLUSIONS AND FUTURE

In this paper I have (*a*) summarized some characteristic qualities of the s.f.R. laser as a spectroscopic tool and (*b*) described a number of outstanding applications of s.f.R. lasers to spectroscopy and pollution detection. In spite of the fact that the s.f.R. laser is not a primary source of tunable laser radiation, it possesses several unique advantages over other tunable laser sources in the infrared. Because of these, the interest in further development of the s.f.R. laser is certain to continue, particularly the search for new materials and pump laser sources to fill the obvious gaps in the s.f.R. laser tuning range. Spectroscopic applications as well as pollution detection application will also flourish. With the availability of a higher efficiency NH_3 laser for converting CO_2 radiation at 9.4 μm to radiation at 12.81 μm, the long wavelength InSb s.f.R. laser is likely to find applications in spectroscopy of UF_6 and perhaps in uranium isotope separation. It appears that we have only seen the beginnings of a promising area of studies.

REFERENCES AND NOTES (Patel)

(1) Melngailis, I. & Mooradian, A. 1975 In *Laser applications in optics and spectroscopy* (ed. S. Jacobs, M. Sargent, J. F. Scott & M. Scully), pp. 1–51. Reading: Addison-Wesley.
(2) Patel, C. K. N. & Shaw, E. D. 1970 *Phys. Rev. Lett.* **24**, 451.
(3) Giordmaine, J. A. & Miller, R. C. 1965 *Phys. Rev. Lett.* **14**, 973. For some recent advances see R. L. Byer in *Tunable Lasers and Applications* (ed. A. Mooradian, T. Jaeger & P. Stokseth), pp. 70–80. Berlin: Springer–Verlag.
(4) Mollenauer, L. F. & Olson, D. H. 1974 *Appl. Phys. Lett.* **24**, 386.
(5) Pine, A. 1974 *J. opt. Soc. Am.* **64**, 1683.
(6) Byer, R. L. & Herbst, R. L. 1977 In *Topics in applied physics: nonlinear infrared generation*, (ed. Y. R. Shen), vol. 16, pp. 81–137. Berlin: Springer–Verlag.
(7) Bridges, T. J. & Nguyen, V. T. 1975 *Appl. Phys. Lett.* **26**, 452; Bridges, T. J., Nguyen, V. T., Burkhardt, E. G. & Patel, C. K. N. *Appl. Phys. Lett.* **27**, 600.
(8) Patel, C. K. N. 1964 *Phys. Rev. Lett.* **12**, 588; **13**, 617.
(9) Patel, C. K. N. 1964 *Appl. Phys. Lett.* **5**, 81; **6**, 12; **7**, 273.

PHILOSOPHICAL TRANSACTIONS OF THE ROYAL SOCIETY A MATHEMATICAL, PHYSICAL & ENGINEERING SCIENCES

(10) Patel, C. K. N., Tien, P. K. & McFee, J. H. 1965 *Appl. Phys. Lett.* **7**, 290. See also a recent review by A. J. DeMaria *Proc. IEEE* **61**, 731 and by O. R. Wood *Proc. IEEE* **62**, 355.
(11) Patel, C. K. N. 1965 *Phys. Rev. Lett.* **15**, 1027.
(12) Patel, C. K. N., Fleury, P. A. & Slusher, R. E. 1966 *Phys. Rev. Lett.* **17**, 1011.
(13) Wolff, P. A. 1966 *Phys. Rev. Lett.* **16**, 225.
(14) Wolff, P. A. 1966 *IEEE J. Quantum Electron.* **QE-2**, 659.
(15) Yafet, Y. 1966 *Phys. Rev.* **152**, 858.
(16) Slusher, R. E., Patel, C. K. N. & Fleury, P. A. 1967 *Phys. Rev. Lett.* **18**, 77.
(17) Patel, C. K. N. 1967 In *Modern optics*, pp. 19–52. New York: Polytechnic Press.
(18) Patel, C. K. N. & Slusher, R. E. 1968 *Phys. Rev.* **167**, 413.
(19) Patel, C. K. N. & Slusher, R. E. 1969 *Phys. Rev.* **117**, 1200.
(20) Pidgeon, C. R. & Smith, S. D. 1977 *Infrared Phys.* **17**, 515.
(21) Mooradian, A., Brueck, S. R. J. & Blum, F. A. 1970 *Appl. Phys. Lett.* **17**, 481.
(22) Patel, C. K. N. 1971 *Appl. Phys. Lett.* **19**, 400.
(23) Patel, C. K. N. 1973 In *Fundamental and applied laser physics* (ed. M. Feld, A. Javan & N. Kurnit), pp. 689–722. New York: John Wiley & Sons.
(24) Patel, C. K. N. 1972 *Phys. Rev. Lett.* **28**, 649.
(25) Brueck, S. R. J. & Mooradian, A. 1974 *IEEE J. Quantum Electron.* **QE-10**, 634.
(26) Thomas, D. G. & Hopfield, J. J. 1968 *Phys. Rev.* **175**, 1021.
(27) Eng, R. S., Mooradian, A. & Fetterman, H. R. 1974 *Appl. Phys. Lett.* **25**, 453.
(28) Scott, J. F. & Damen, T. C. 1972 *Phys. Rev. Lett.* **29**, 107; S. Geschwind, R. Romestain, P. Hu & T. Jedju *J. Semicond. Insulators* (to be published, 1978).
(29) Weber, B. A., Sattler, J. P. & Nemarich, J. 1975 *Appl. Phys. Lett.* **27**, 93.
(30) Patel, C. K. N., Chang, T. Y. & Nguyen, V. T. 1976 *Appl. Phys. Lett.* **28**, 603.
(31) Chang, T. Y. & McGee, J. D. 1976 *Appl. Phys. Lett.* **28**, 526.
(32) Patel, C. K. N., Slusher, R. E., Fleury, P. A. & Frisch, H. L. 1966 *Phys. Rev. Lett.* **16**, 971.
(33) Al-Watban, F. A., Harrison, R. G., Crowder, J. G. & Pidgeon, C. R. 1977 *J. Phys.* D **10**, L167.
(34) Harrison, R. G., Al-Watban, F. A. & Pidgeon, C. R. 1977 *Opt. Communs* **23**, 385.
(35) Brueck, S. R. J. & Mooradian, A. 1976 *IEEE J. Quantum Electron.* **QE 12**, 201.
(36) Scragg, T. & Smith, S. D. 1975 *Opt. Communs* **15**, 166.
(37) Scragg, T., Ironside, C. N., Dennis, R. B. & Smith, S. D. 1976 *Opt. Communs* **18**, 456.
(38) DeSilets, C. S. & Patel, C. K. N. 1973 *Appl. Phys. Lett.* **22**, 543.
(39) Brueck, S. R. J. & Mooradian, A. 1973 *Opt. Communs* **8**, 263.
(40) Bell, A. G. 1881 *Phil. Mag.* **11**, 510; J. Tyndall, 1881 *Proc. R. Soc. Lond.* A **31**, 307; W. C. Rontgen, 1881 *Phil. Mag.* **11**, 308.
(41) Patel, C. K. N., Shaw, E. D. & Kerl, R. J. 1970 *Phys. Rev. Lett.* **25**, 8.
(42) Patel, C. K. N. 1973 In *Coherence and Quantum optics* (ed. L. Mandel & E. Wolff), pp. 507–593. New York: Plenum Press.
(43) Guerra, M. A., Brueck, S. R. J. & Mooradian, A. 1973 *IEEE J. Quantum Electron.* **QE 9**, 1157.
(44) Smith, S. D. 1976 In *Very high resolution spectroscopy* (ed. R. A. Smith), pp. 13–49. New York: Academic Press.
(45) Nowakowski, A. Z., Dennis, R. B., Scragg, T. Hamza, F. H. & Smith, S. D. 1976 *Opt. Laser Technol.*, p. 133.
(46) Patel, C. K. N. 1974 In *Laser spectroscopy* (ed. R. G. Brewer & A. Mooradian), pp. 471–491. New York: Plenum Press.
(47) Colles, M. J. & Pidgeon, C. R. 1975 *Rep. Prog. Phys.* **38**, 329.
(48) Patel, C. K. N. 1974 *Appl. Phys. Lett.* **25**, 112.
(49) Blum, F. A., Nill, K. W., Calawa, A. R. & Harman, T. C. 1972 *Chem. Phys. Lett.* **15**, 144.
(50) Kerr, E. L. & Atwood, J. G. 1968 *Appl. Opt.* **7**, 915.
(51) Kreuzer, L. B. 1971 *J. appl. Phys.* **42**, 2934.
(52) Kreuzer, L. B. & Patel, C. K. N. 1971 *Science, N.Y.* **173**, 45.
(53) Patel, C. K. N. (in preparation).
(54) Patel, C. K. N. & Kerl, R. J. 1977 *Appl. Phys. Lett.* **30**, 578.
(55) Keck, D. B. 1969 Ph.D. Thesis, Michigan State University (unpublished). P. G. Favero, A. M. Mirri, and W. Gordy *Phys. Rev.* **114**, 1534.
(56) Patel, C. K. N. & Kerl, R. J. *Opt. Communs* (to be published).
(57) Patel, C. K. N., (unpublished).
(58) For low pressure ($P < 200$ mTorr) o.a. spectra see ref. (53).
(59) Nill, K. W., Blum, F. A., Calawa, A. R. & Harman, T. C. 1972 *Chem. Phys. Lett.* **14**, 234.
(60) Bridges, T. J. & Burkhardt, E. G. 1977 *Opt. Communs* **22**, 248.
(61) Guerra, M. A., Sanchez, A. & Javan, A. 1977 *Phys. Rev. Lett.* **38**, 482.
(62) Patel, C. K. N., Kerl, R. J. & Burkhardt, E. G. 1977 *Phys. Rev. Lett.* **38**, 1204.
(63) Amiot, C., Bacis, R. & Guelachvili, G. *Can. J. Phys.* (to be published).

PHILOSOPHICAL TRANSACTIONS OF THE ROYAL SOCIETY A MATHEMATICAL, PHYSICAL & ENGINEERING SCIENCES

(64) Patel, C. K. N. 1978 *Phys. Rev. Lett.* **40**, 535.
(65) Olman, M. D., McNelis, M. D. & Hause, C. D. 1964 *J. molec. Spectrosc.* **14**, 62.
(66) Patel, C. K. N. (in preparation).
(67) Johnston, H. L. 1973 *Science, N.Y.* **173**, 517.
(68) Crutzen, P. J. 1971 *J. geophys. Res.* **76**, 7311.
(69) Patel, C. K. N., Burkhardt, E. G. & Lambert, C. A. 1974 *Science, N.Y.* **184**, 1173; E. G. Burkhardt, C. A. Lambert & C. K. N. Patel 1975 *Science, N.Y.* **188**, 1111; C. K. N. Patel 1976 *Opt. quantum Electronics* **8**, 145.
(70) Chaloner, C. P., Drummond, J. R., Houghton, J. T., Jarnot, R. F. & Roskoe, H. K. 1975 *Nature, Lond.* **258**, 696.

PHILOSOPHICAL TRANSACTIONS OF THE ROYAL SOCIETY A MATHEMATICAL, PHYSICAL & ENGINEERING SCIENCES

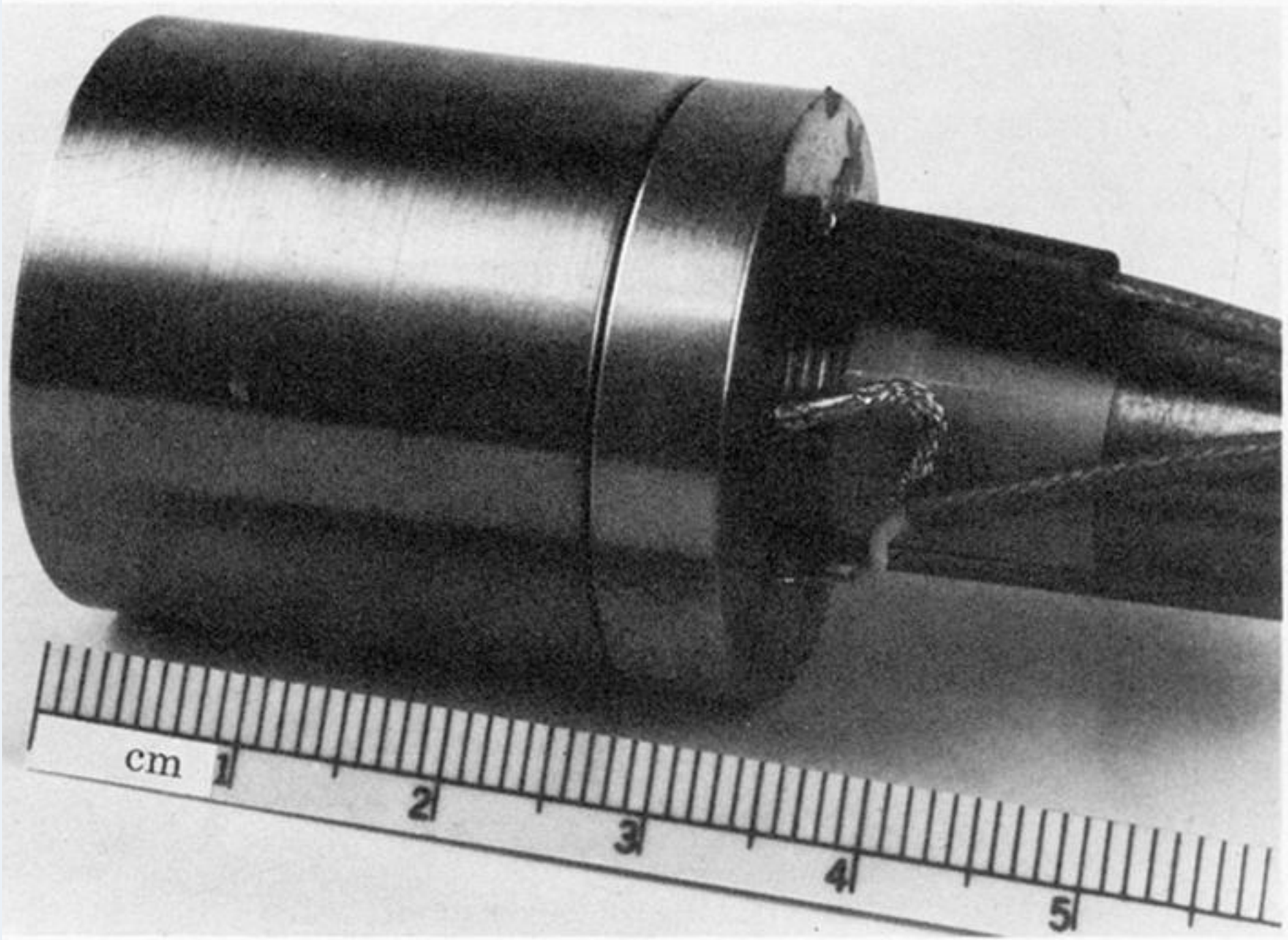

FIGURE 8. Miniature o.a. absorption cell.